

Fig. 4.13 Velocity vectors on the cross plane $\theta = 0^\circ$ & 180° at steady state for $D_j = 10.0$ mm, $H = 10.0$ mm, $Ra = 940$ ($\Delta T = 10^\circ\text{C}$) for $Re_j =$ (a) 135 ($Q_j=1.0$ slpm), (b) 270 ($Q_j=2.0$ slpm), (c) 406 ($Q_j=3.0$ slpm), (d) 541 ($Q_j=4.0$ slpm), and (e) 676 ($Q_j=5.0$ slpm).

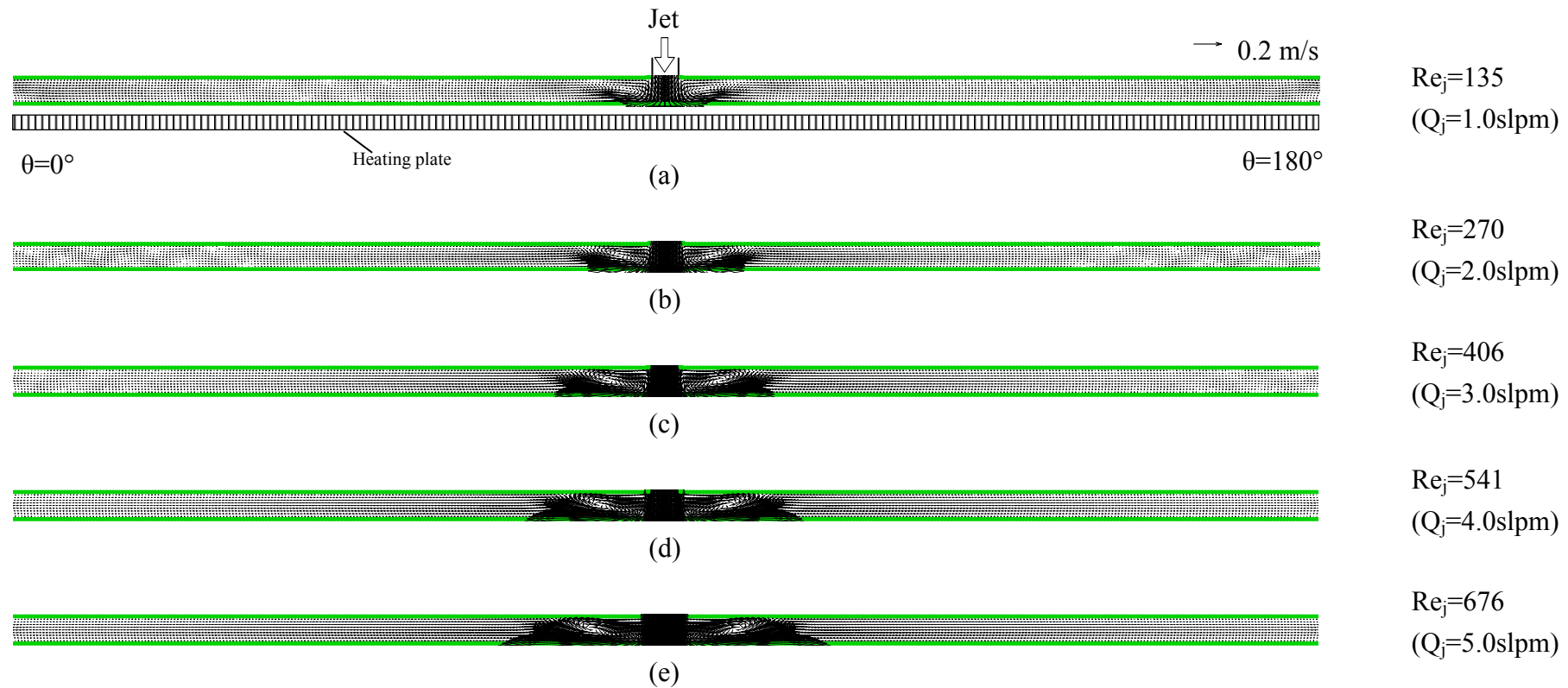


Fig. 4.14 Velocity vectors on the cross plane $\theta = 0^\circ$ & 180° at steady state for $D_j = 10.0 \text{ mm}$, $H = 10.0 \text{ mm}$, $Ra = 1,409$ ($\Delta T = 15.0^\circ\text{C}$) for $Re_j =$ (a) 135 ($Q_j=1.0 \text{ slpm}$), (b) 270 ($Q_j=2.0 \text{ slpm}$), (c) 406 ($Q_j=3.0 \text{ slpm}$), (d) 541 ($Q_j=4.0 \text{ slpm}$), and (e) 676 ($Q_j=5.0 \text{ slpm}$).

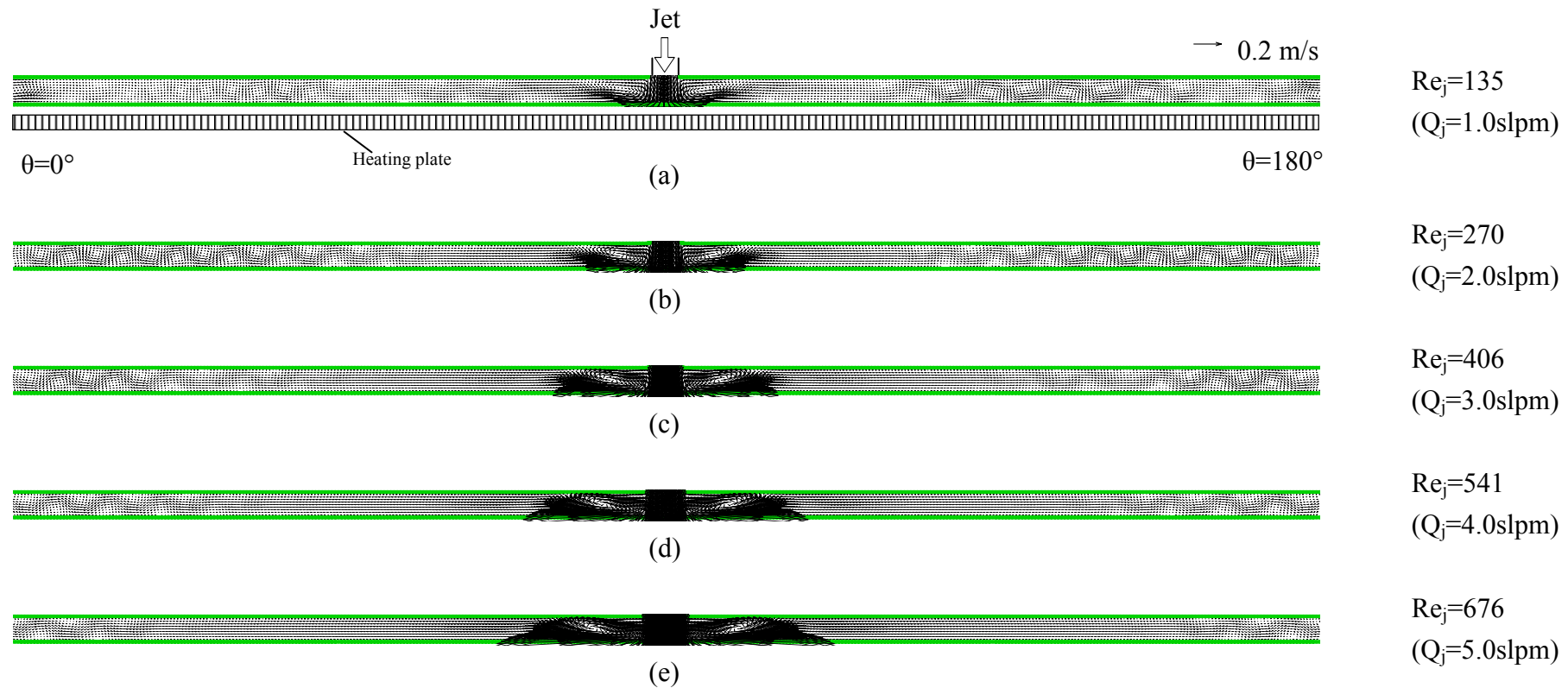


Fig. 4.15 Velocity vectors on the cross plane $\theta = 0^\circ$ & 180° at steady state for $D_j = 10.0 \text{ mm}$, $H = 10.0 \text{ mm}$, $Ra = 1,880$ ($\Delta T = 20.0^\circ\text{C}$) for $Re_j =$ (a) 135 ($Q_j=1.0 \text{ slpm}$), (b) 270 ($Q_j=2.0 \text{ slpm}$), (c) 406 ($Q_j=3.0 \text{ slpm}$), (d) 541 ($Q_j=4.0 \text{ slpm}$), and (e) 676 ($Q_j=5.0 \text{ slpm}$).

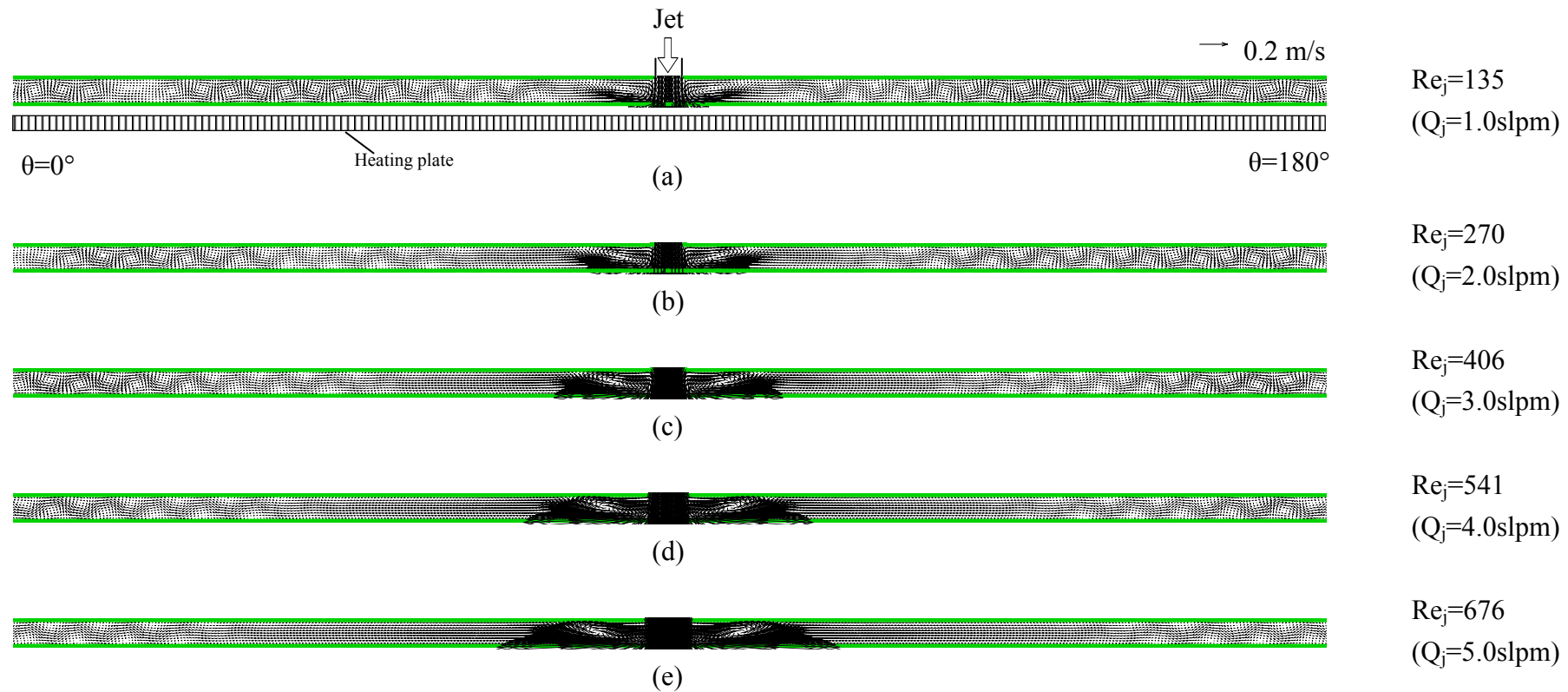


Fig. 4.16 Velocity vectors on the cross plane $\theta = 0^\circ$ & 180° at steady state for $D_j = 10.0$ mm, $H = 10.0$ mm, $Ra = 2,348$ ($\Delta T = 25.0^\circ\text{C}$) for $Re_j =$ (a) 135 ($Q_j = 1.0$ slpm), (b) 270 ($Q_j = 2.0$ slpm), (c) 406 ($Q_j = 3.0$ slpm), (d) 541 ($Q_j = 4.0$ slpm), and (e) 676 ($Q_j = 5.0$ slpm).

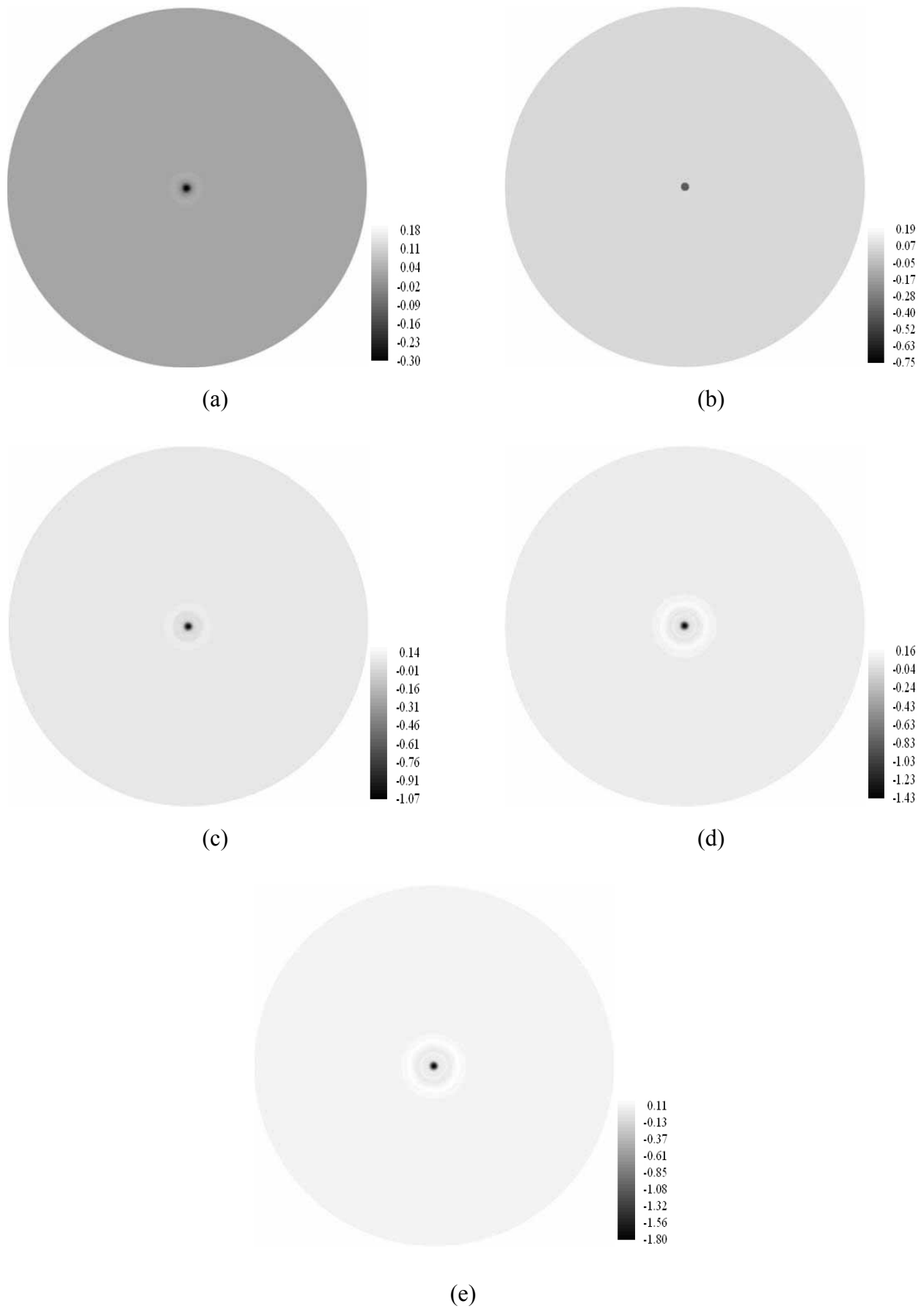


Fig. 4.17 Contours of vertical velocity component w at long time at the horizontal plane $z = -5$ mm for $Ra = 470$ ($\Delta T = 5.0^\circ\text{C}$) and $D_j = 10.0\text{mm}$ at $H = 10.0$ mm for $Re_j =$ (a) 135, (b) 270, (c) 406, (d) 541, and (e) 676.

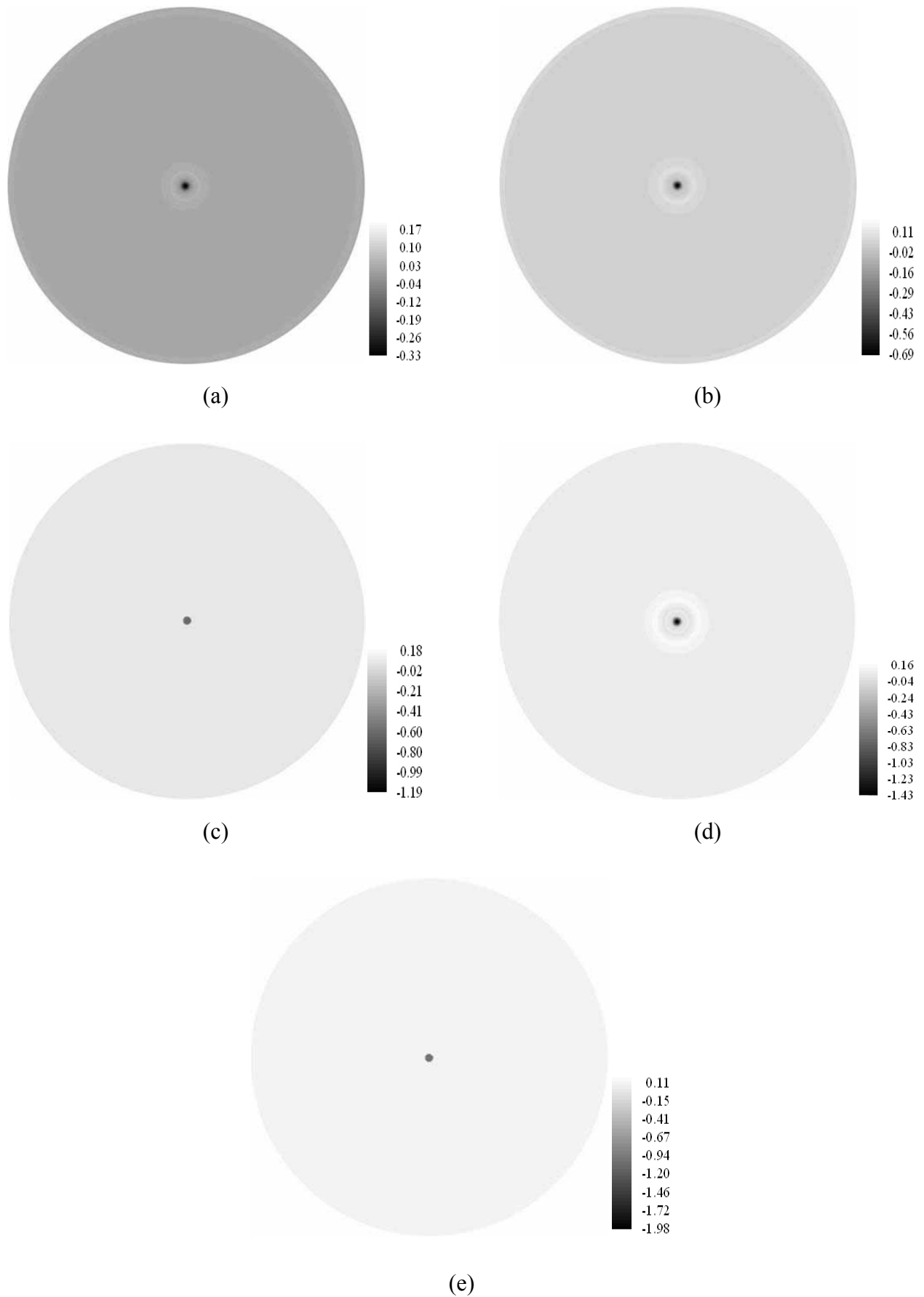


Fig. 4.18 Contours of vertical velocity component w at long time at the horizontal plane $z = -5$ mm for $Ra = 940$ ($\Delta T = 10.0^\circ\text{C}$) and $D_j = 10.0\text{mm}$ at $H = 10.0$ mm for $Re_j =$ (a) 135, (b) 270, (c) 406, (d) 541, and (e) 676.

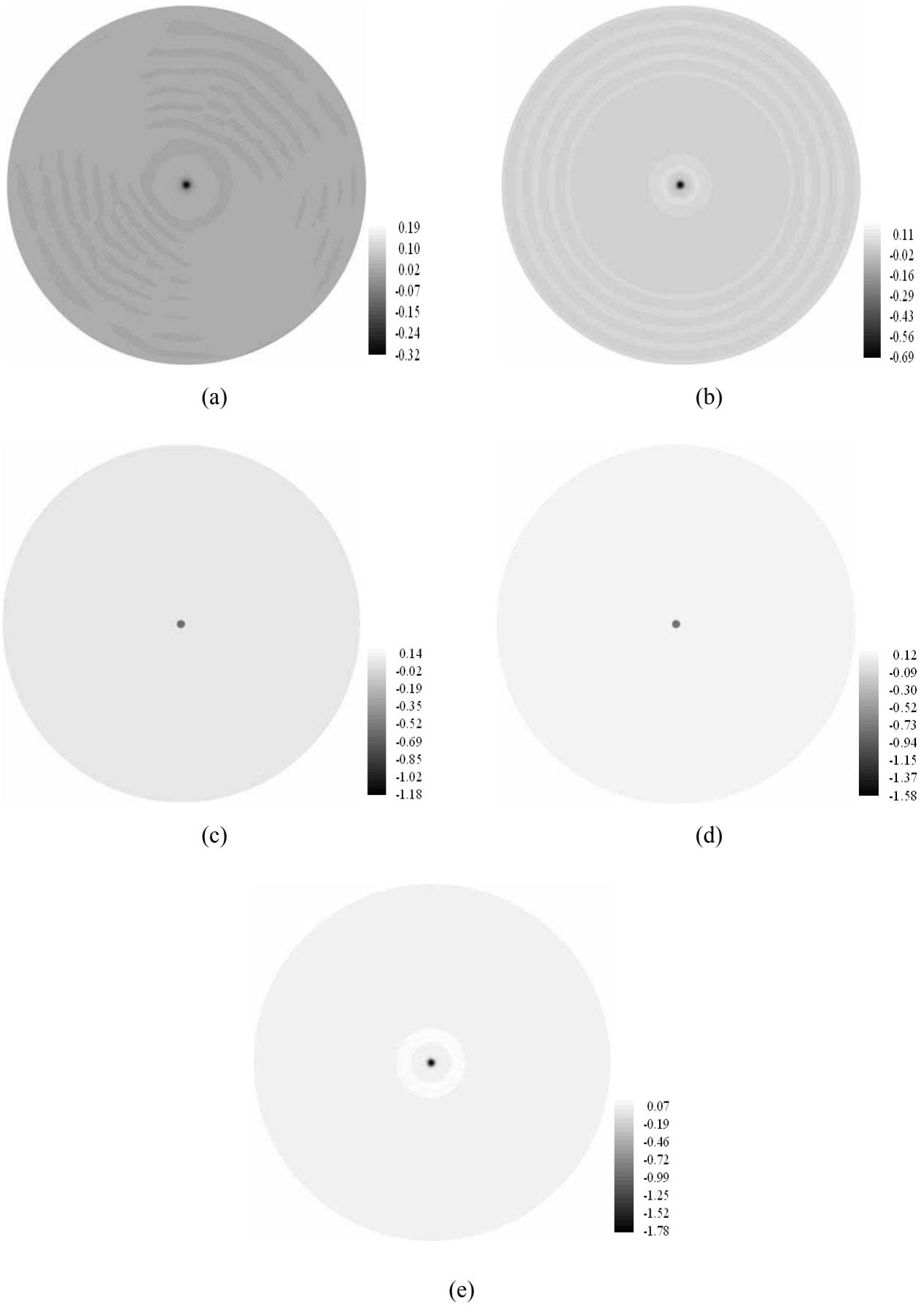


Fig. 4.19 Contours of vertical velocity component w at long time at the horizontal plane at $z = -5$ mm for $Ra = 1,409$ ($\Delta T = 15.0^\circ C$) and $D_j = 10.0$ mm at $H = 10.0$ mm for $Re_j =$ (a) 135, (b) 270, (c) 406, (d) 541, and (e) 676.

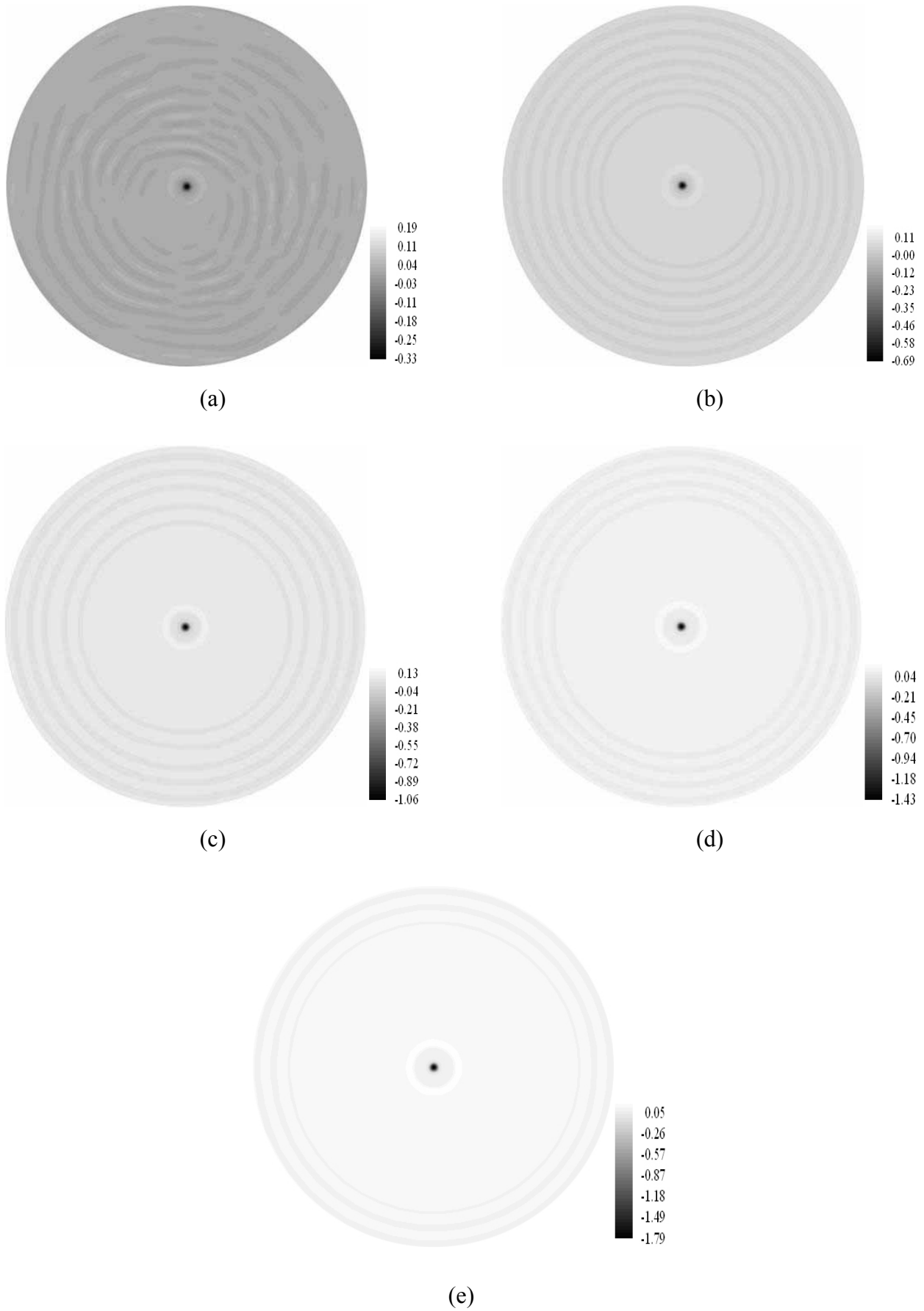


Fig. 4.20 Contours of vertical velocity component w at long time at the horizontal plane at $z = -5$ mm for $Ra = 1,880$ ($\Delta T = 20.0^\circ\text{C}$) and $D_j = 10.0\text{mm}$ at $H = 10.0$ mm for $Re_j =$ (a) 135, (b) 270, (c) 406, (d) 541, and (e) 676.

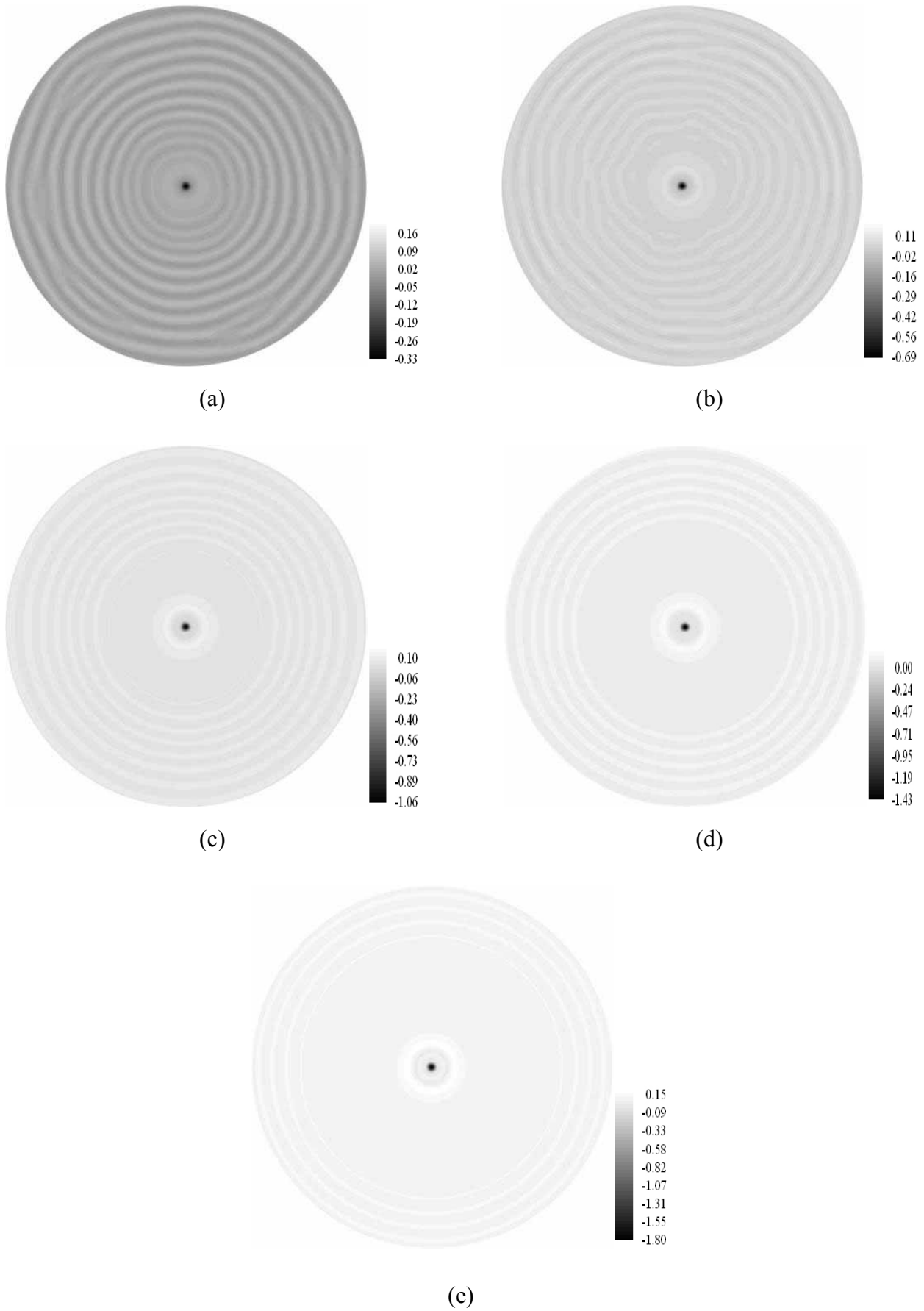


Fig. 4.21 Contours of vertical velocity component w at long time at the horizontal plane at $z = -5$ mm for $Ra = 2,348$ ($\Delta T = 25.0^\circ\text{C}$) and $D_j = 10.0\text{mm}$ at $H = 10.0$ mm for $Re_j =$ (a) 135, (b) 270, (c) 406, (d) 541, and (e) 676.

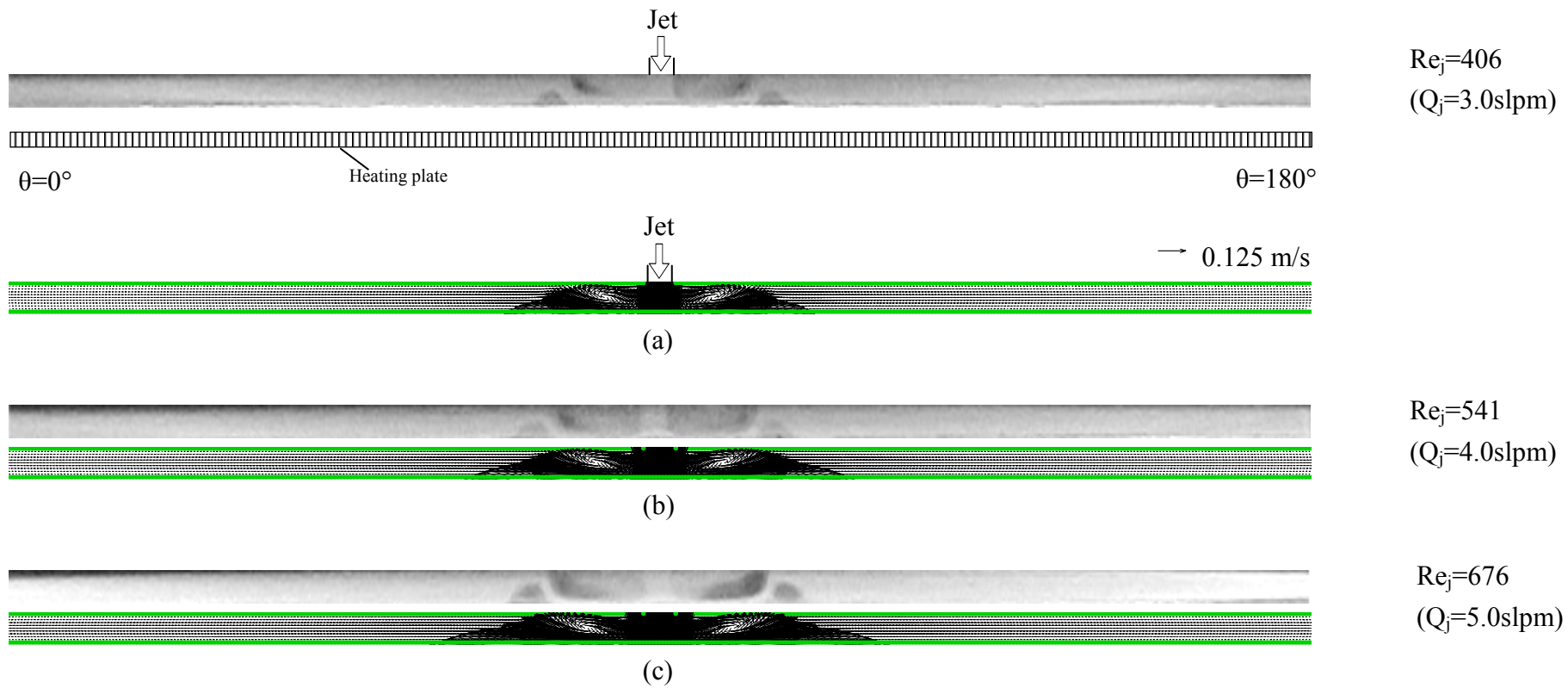


Fig. 4.22 Steady side view flow photo on the cross plane $\theta = 0^\circ$ & 180° from Hsieh and Lin [36] and predicted velocity vectors from the present study on the same plane for $D_j = 10.0 \text{ mm}$, $H = 10.0 \text{ mm}$, $Ra = 470$ ($\Delta T = 5^\circ\text{C}$) for $Re_j =$ (a) 406 ($Q_j=3.0 \text{ slpm}$), (b) 541 ($Q_j=4.0 \text{ slpm}$), and (c) 676 ($Q_j=5.0 \text{ slpm}$).